

# Ridge push, mantle plumes and the speed of the Indian plate

Graeme Eagles<sup>1,2</sup> and Affelia D. Wibisono<sup>3</sup>

<sup>1</sup>Department of Earth Sciences, Royal Holloway University of London, Egham, Surrey TW20 0EX, UK. E-mail: graeme.eagles@rhul.ac.uk

<sup>2</sup>Alfred Wegener Institute for Polar and Marine Research, Am Alten Hafen 26, 27568 Bremerhaven, Germany. E-mail: graeme.eagles@awi.de

<sup>3</sup>Department of Physics, Royal Holloway University of London, Egham, Surrey TW20 0EX, UK

Accepted 2013 April 17. Received 2013 April 15; in original form 2012 November 12

## SUMMARY

The buoyancy of lithospheric slabs in subduction zones is widely thought to dominate the torques driving plate tectonics. In late Cretaceous and early Paleogene times, the Indian plate moved more rapidly over the mantle than freely subducting slabs sink within it. This signal event has been attributed to arrival of the Deccan–Réunion mantle plume beneath the plate, but it is unknown in which proportions the plume acted to alter the balance of existing plate driving torques and to introduce torques of its own. Our plate kinematic analysis of the Mascarene Basin yields a detailed Indian plate motion history for the period 89–60 Ma. Plate speed initially increases steadily until a pronounced acceleration in the period 68–64 Ma, after which it abruptly returns to values much like those beforehand. This pattern is unlike that suggested to result from the direct introduction of driving forces by the arrival of a thermal plume at the base of the plate. A simple analysis of the gravitational force related to the Indian plate's thickening away from its boundary with the African plate suggests instead that the sudden acceleration and deceleration may be related to uplift of part of that boundary during a period when it was located over the plume head. In this instance, torques related to plate accretion and subduction may have contributed in similar proportions to drive plate motion.

**Key words:** Plate motions; Magnetic anomalies: modelling and interpretation; Mid-ocean ridge processes; Dynamics: gravity and tectonics; Hotspots; Indian Ocean.

## INTRODUCTION

Plate tectonics is of fundamental importance to the Earth system, and yet there is no consensus on the balance of torques that drives it. Of the measurable constraints on this balance, intraplate stress correlates with calculations of the gravitational torque related to plate thickening ('ridge push'), whereas plate speed correlates with the lengths of subduction zones at which subduction-related torques ('slab pull') are generated (Coblenz & Richardson 1995). Furthermore, slab buoyancy, the dominant contributor to slab pull, is estimated to be the greater torque by an order of magnitude, and thus is widely expected to dominate in driving plate motion (Forsyth & Uyeda 1975). Consistent with this, rates of plate motion have rarely exceeded estimates of the maximum sinking rate of slabs in the upper mantle (Goes *et al.* 2008).

A unique exception to this pattern is a period of rapid motion by the Indian plate in late Cretaceous and Paleogene times. This event coincides with the Deccan Traps volcanic episode and so has been related to processes occurring during the arrival and spread of the Deccan–Réunion mantle plume. In one view, the plume reduces viscous drag on the base of the Indian plate so that it can be driven faster by slab pull (Kumar *et al.* 2007). In another, the outwards-spreading plume mantle itself drags the plate by virtue of their viscous coupling, at the same time as which a so-called 'downhill' force sees the plate migrate away from the geoid high centred on

the plume head (Gurnis & Torsvik 1994; Becker & Faccenna 2011; Cande & Stegman 2011; van Hinsbergen *et al.* 2011).

To understand the contributions of these effects more fully, we generate a detailed record of Indian plate motion over the mantle in late Cretaceous and Paleogene times. Currently, the onset and early history of the rapid motion event is not characterized at high resolution because of slow divergence in the African–Antarctic arm of the plate circuit with Antarctica that available models of Indian–African plate divergence are built from (Molnar *et al.* 1988; Cande *et al.* 2010). Study of the seafloor spreading record in the Mascarene and Laxmi basins promises greater resolution because they opened in the context of what came to be faster Africa–India divergence (Bernard & Munschy 2000).

## THE MASCARENE BASIN

The Mascarene Basin occupies the part of the Indian Ocean immediately east of Madagascar. Seafloor spreading there created a sequence of late Cretaceous to early Paleogene magnetic isochrons that are widely and consistently identified in the range of 34°–26° (Dymond 1991; Bernard & Munschy 2000). The basin's western limit is the north–northeast-striking continental margin of Madagascar, which is straight and exceeds 1000 km in length (Fig. 1). A positive–negative gravity anomaly couplet suggests that the margin

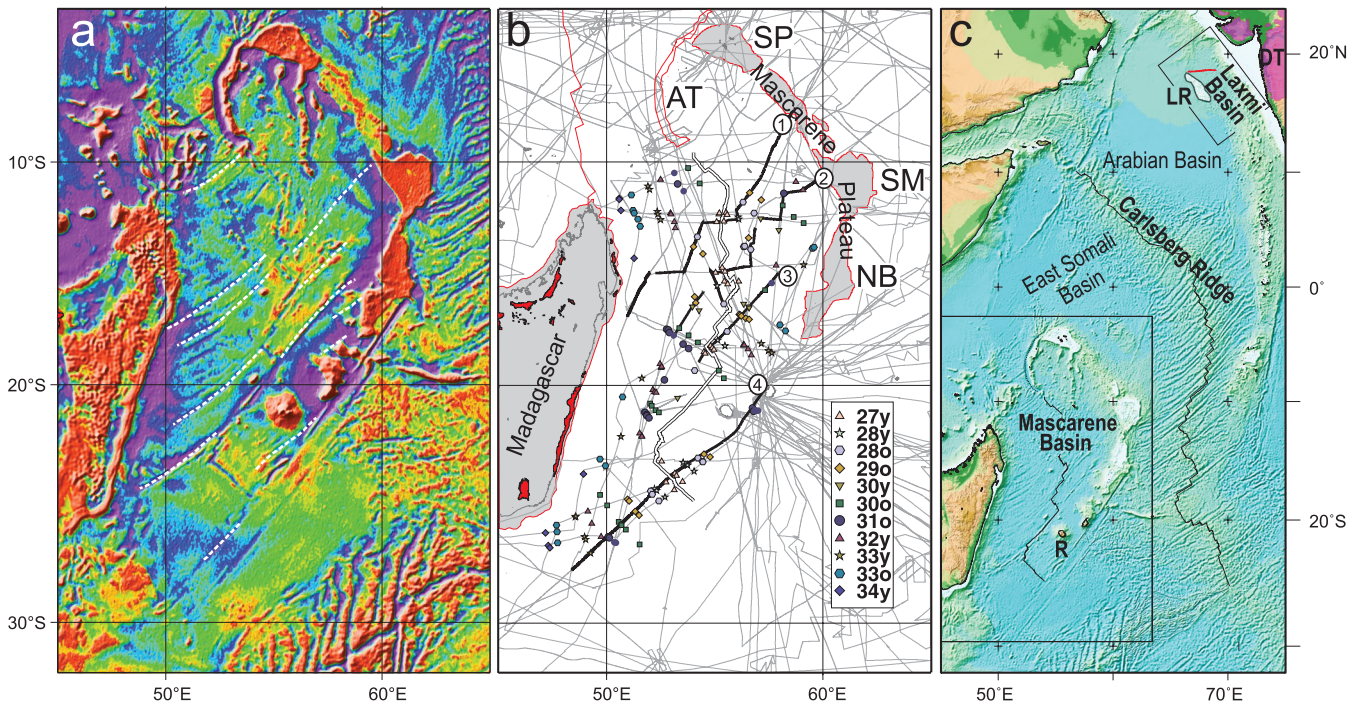


**Figure 1.** (a) Satellite-derived free-air gravity data in the Mascarene Basin. White lines: interpreted fracture zone traces. (b) Magnetic isochron interpretations and data set. Coloured symbols: picks of magnetic anomalies (labels in the key bottom right). Grey lines: NGDC archive magnetic data profiles. Numbered black lines: composite magnetic profiles in Fig. 2. Double black line: median valley of the extinct African–Indian ridge in the Mascarene Basin. Red: breakup-related Morondava volcanics dating from 89 Ma (Storey *et al.* 1997). AT: Amirante Trench, NB: Nazareth Bank, SM: Saya da Malha Bank, SP: Seychelles Plateau. (c) The NW Indian Ocean. DT: Deccan Traps, LR: Laxmi Ridge; R: current location of the Réunion hotspot. Red line: profile in Fig. 4.

hosts a strip of extended continental crust. Transform motion dating from before the opening of the Mascarene Basin has been suggested as responsible for the linearity of the shelf, but its details are controversial (e.g. Lawver *et al.* 1998; Torsvik *et al.* 2008). Onshore, the margin hosts the so-called Morondava province of Cretaceous ( $\sim 89$  Ma) igneous rocks that are attributed to the action of the same mantle plume as the present-day Marion hot spot (Storey *et al.* 1997; Fig. 1).

Continental basement is exposed on the Seychelles islands at the basin's eastern margin in the form of Precambrian granites (Torsvik *et al.* 2001). The islands lie at the northern end of a broad and continuous submarine ridge called the Mascarene Plateau (Fig. 1). Drilling on the southern parts of the plateau returned Cenozoic basalts at Saya de Malha and Nazareth banks, which were concluded to have been emplaced during the passage of the Deccan–Réunion plume close to the basin margin (Duncan & Hargraves 1990). The nature of the basement to this basalt is not directly known. During its final growth after chron 28 (64 Ma), northeastern parts of the basin moved independently as part of a separate Seychelles plate whose size, shape and kinematics are only now becoming known (Cande *et al.* 2010; Ganerød *et al.* 2011; Eagles & Hoang in review). In particular, it is now clear that the plate's western boundary occupied the 5.2–5.7 km deep Amirante Trench.

Observing these geographical constraints, we digitised NE-trending fracture zones in satellite-derived gravity data (Sandwell & Smith 2009), extending away from offsets on an abandoned SE-striking mid-ocean ridge nearly all the way to the continental shelf of Madagascar (Fig. 1). Fracture zones of the eastern half of the basin are less prominent in these data, perhaps owing to effects of the same volcanic episodes that built the Mascarene Plateau on the basin's eastern margin. In magnetic anomaly data, the re-

versed polarity part of anomaly 26 envelopes a median valley at the ridge crest suggesting its abandonment during intermediate to slow seafloor spreading at some point in the period 61.1–58.74 Ma (Gradstein *et al.* 2004). The northern part of the median valley is sinuous between 13.5°S and 10.5°S. North of this point, the youngest seafloor is characterized by the presence of magnetic anomaly 30 on the west flank of the median valley. The basin is characterized by coherent but asymmetrical sequences of magnetic anomalies, indicating growth by organized spreading that was punctuated by ridge jumps or propagations. We interpreted these anomalies using a scheme with minimal spreading rate changes, model ridge jumps and propagations (Fig. 2). This scheme and the resulting set of isochron picks differ slightly in its youngest parts from previous ones (Bernard & Munschy 2000), so as not to imply propagating extinction of the Mascarene Ridge. The advantage of this scheme is that it does not require multiple unattested transform faults to connect the retreating tip of a dying Mascarene ridge to the Carlsberg Ridge.

Our India–Africa rotation parameters (Table 1; Fig. 3) derive from iterative least-squares fitting of the fracture zone and magnetic isochron data (Eagles 2003; Livermore *et al.* 2005). Individual whole fracture zones are fitted to synthetic ridge-crest offset flow-lines that are generated from the finite rotations. Magnetic anomaly picks are fitted by rotation to great circle segments defined from their conjugate and non-conjugate neighbours within shared corridors of crust produced by the action of individual ridge crest segments. Initially, we fitted conjugate magnetic anomalies only to minimize the effects of spreading asymmetry on the solution rotations, before carefully introducing data without conjugates. The solution produces a good visual approximation of the data (Fig. 3). The moderately large 95 per cent confidence ellipses surrounding

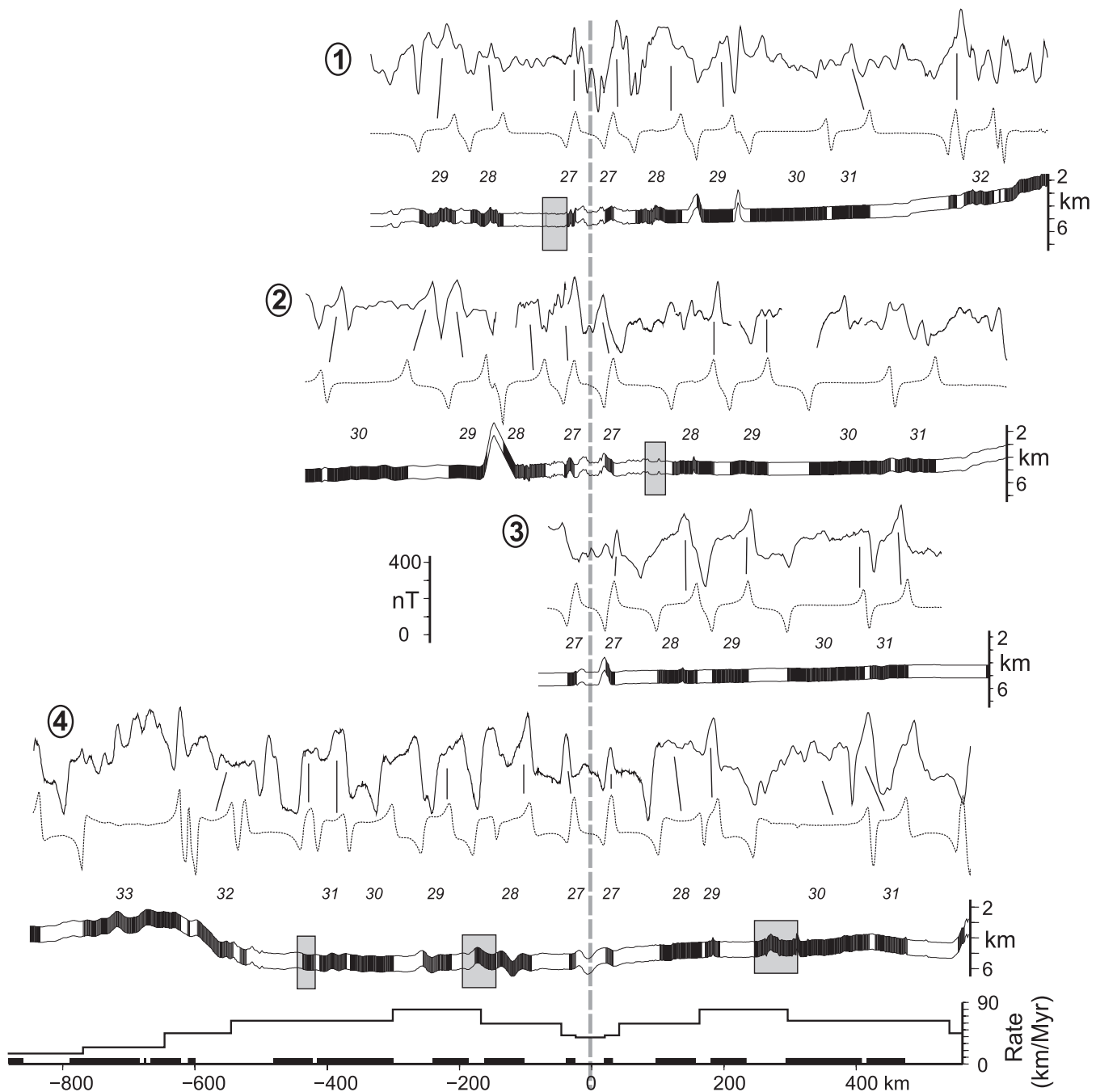


**Figure 2.** Four magnetic anomaly profiles (numbered solid lines, locations in Fig. 1) and anomaly isochron models (dashed lines) for them in the Mascarene Basin. Models use a 1-km-thick source layer with its upper surface at the bathymetry (depth in km) along the profile. Model spreading rate variations at the bottom of the figure. Normal and reverse-polarity seafloor magnetization is shown by the black and white blocks within the model layer. Segments of this block model that have been transferred from one flank to the opposing flank by ridge crest jumps or propagations are highlighted by grey boxes.

the rotation parameters primarily reflect the shortness of the Mascarene Ridge. Quantitatively, standard deviations are 3.36 km for misfits to synthetic flowlines, and 11.67 km to isochron targets. The larger latter figure is mostly a consequence of non-conjugate fitting with lone picks, which are less reliably identifiable than picks in groups, but necessary in view of the overall paucity of picks for some isochrons. By the latter stages of the inversion, these data come to be weighted so that they have little influence on the stability of the overall solution.

Motion of the Seychelles plate in the northeastern part of the Mascarene Basin occurred independently of the motion of the African

and Indian plates that produced the southern parts of the basin. If any of the data in our model had formed at a plate boundary with the Seychelles plate or at the Africa–India boundary and were subsequently rotated by that plate’s motion, they would appear as large misfits to the predictions of our two-plate model. There is no clustering of large misfits in the northeastern parts of our data set to suggest that this may have occurred. The Seychelles plate must therefore have been small and confined to the northernmost Mascarene Basin beyond the area covered by our data. We are confident that the rotations can be used to accurately describe Indian–African plate divergence.

**Table 1.** Rotation parameters (India with respect to Africa until Mascarene Basin abandonment) and 95 per cent confidence regions. The 120–61 Ma rotation is constructed using the 120 Ma rotation from Torsvik *et al.* (2008) and an interpolated 61 Ma rotation from Eagles & Hoang (in review).

Model	Rotation	Parameters	1 $\sigma$ ellipsoid axes (great circle degrees)			Ellipsoid azimuth, degrees clockwise of N	Magnetic timescale label and pick	Timescale Age (Ma)
			Longitude	Latitude	Angle	1	2	3
–163.75	–15.91	0.0	—	—	—	—	Extinction	61.0
–163.66	–15.99	0.57	7.68	0.29	0.046	42.39	27n (young edge)	61.65
–160.76	–18.09	2.06	7.25	0.62	0.078	46.41	28n (young edge)	63.10
–161.82	–17.26	3.05	4.83	0.46	0.069	44.76	28n (old edge)	64.13
–162.41	–17.11	5.06	2.87	0.24	0.070	44.21	29n (old edge)	65.12
–158.30	–15.06	6.94	1.92	0.17	0.068	45.28	30n (young edge)	65.86
–158.93	–16.73	9.59	1.78	0.13	0.052	42.34	30n (old edge)	67.70
–160.06	–18.51	10.27	1.46	0.13	0.046	42.96	31n (old edge)	68.73
–160.67	–20.29	11.96	1.33	0.12	0.046	43.72	32n.1n (young edge)	70.96
–162.39	–22.42	13.12	1.45	0.12	0.063	42.49	33n (young edge)	73.58
–171.23	–31.59	13.58	1.90	0.11	0.060	40.81	33n (old edge)	79.54
–175.05	–34.93	14.28	2.27	0.16	0.069	38.94	34n (young edge)	84.00
–179.22	–38.15	15.16	—	—	—	—	FIT	89.0
–133.98	–23.33	19.83	—	—	—	—	From Torsvik <i>et al.</i> (2008)	120

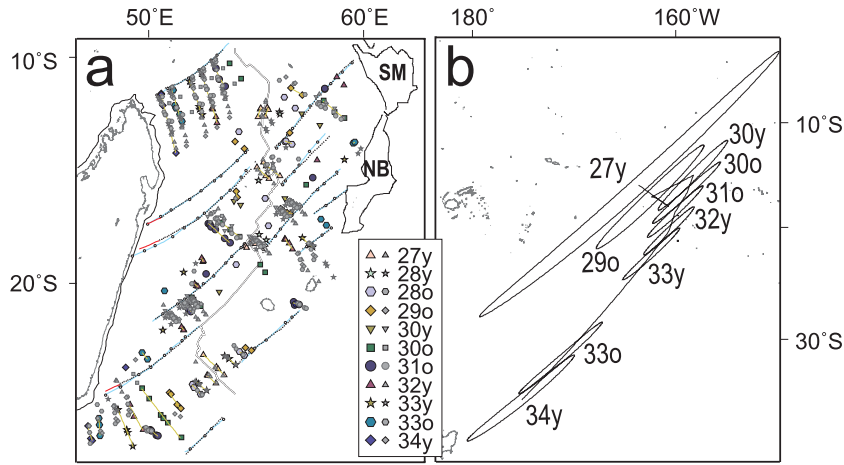


**Figure 3.** (a) model fits. Small grey symbols: rotated conjugate and non-conjugate magnetic isochron picks, grey lines with white points: synthetic flowlines, small black triangles: picks along the fracture zones shown as lines in Fig. 1. Red lines: extensions of these fracture zones between anomaly 34y and the continental margin of Madagascar. (b) Finite rotation poles and selected (for clarity) 95 per cent confidence ellipses. Figure altered to make synthetic flowlines and FZ picks more easy to compare to one another. The synthetic flowlines are plotted in a lighter blue and the synthetic flowpoints are shown by smaller disks. SM: Salha da Maya Bank, NB: Nazareth Bank.

The strike of fracture zones continues unchanged beyond anomaly 34y picks towards the continental margin of Madagascar. Extrapolation of synthetic flowlines to match these features, using the same rotation rate prior to chron 34y as immediately after it, enables us to produce a total reconstruction rotation (labelled FIT in Table 1) and estimate the onset of extension at  $\sim 89$  Ma. Uncertainty in this rotation cannot be quantified as there is no 89 Ma isochron to constrain it, but the good visual fit to the early fracture zones and the presence of widespread  $\sim 89$  Ma breakup-related Morondava volcanic rocks on Madagascar provides some qualitative confidence (Storey *et al.* 1997; Fig. 1). On the Indian side of the basin, the synthetic flowlines terminate towards the Mascarene Plateau at the western margin of its southern reach, Nazareth Bank and within its northern part, Saya da Malha Bank. Barring significant basinwide asymmetry in crustal accretion prior to chron 33o (anomaly 34y is

only recorded on the African side of the basin), this indicates that the basement to the banks, beneath their Cenozoic basalt mantles, did not form by oceanic crustal accretion in the Mascarene Basin. Alternative interpretations of this basement are that it may be continental or transitional in nature, as recently suggested by Torsvik *et al.* (2013), making it conjugate to the eastern Madagascar margin, or that it formed during oceanic crustal accretion to the Carlsberg Ridge.

## THE LAXMI BASIN

Two microcontinents, the Seychelles platform and Laxmi Ridge, became isolated in a shared corridor of Indian–African plate divergence by geologically-rapid relocations of part of the Indian

plate's southwestern divergent boundary. This phenomenon has been related to weakening of the Indian continental margin by the Deccan–Réunion plume (Müller *et al.* 2001). The microcontinents consequently separate parts of three oceanic basins: the northern Mascarene, Arabian–East Somali and Laxmi basins (Fig. 1). The oldest seafloor in the Arabian–East Somali Basin dates from the normal polarity part of chron 28 (Masson 1984; Collier *et al.* 2008). The youngest seafloor in the northern Mascarene Basin dates from the normal polarity part of chron 30 (Bernard & Munschy 2000); its location south of the Amirante Trench makes it implausible to interpret that any younger seafloor in the basin was lost to the subduction that is inferred to have occurred at the trench (Cande *et al.* 2010). Consequently, at least the products of chron 30y–28o aged plate divergence, at somewhat more than 200 km (Cande *et al.* 2010; Eagles & Hoang in review), must exist to be accounted for in the corridor.

The obvious location for this material is the Laxmi Basin. Linear magnetic anomalies within the basin have been interpreted to have formed by ultra slow seafloor spreading between chronos 33 and 28 (Bhattacharya *et al.* 1994). However, the basin's axial volcanic plug, lack of fracture zones and smooth seismic basement surface (Krishna *et al.* 2006; Corfield *et al.* 2010) are more consistent with faster spreading and/or the vigorous melt production implied by proximity to the mantle plume head, which was supplying the adjacent Deccan Traps between chronos 30 and 28. Consistent with this, Fig. 4 illustrates that the basin's magnetic data can be modelled as showing anomalies 29 and 28 in oceanic crust that formed at fast divergence rates, and with a closer resemblance than to a slow spreading model like Bhattacharya *et al.*'s (1994). In detail, it is not possible to rule out the possibilities that these magnetic anomalies betray susceptibility contrasts within or at the edges of transitional (rather than oceanic) crust in the basin floor, but we note that this does not preclude identification of those anomalies as isochrons (Bridges *et al.* 2012). We conclude that a simple and therefore persuasive view of these data is as indications of a Laxmi Basin that had evolved to a site of oceanic accretion during chronos 29 and

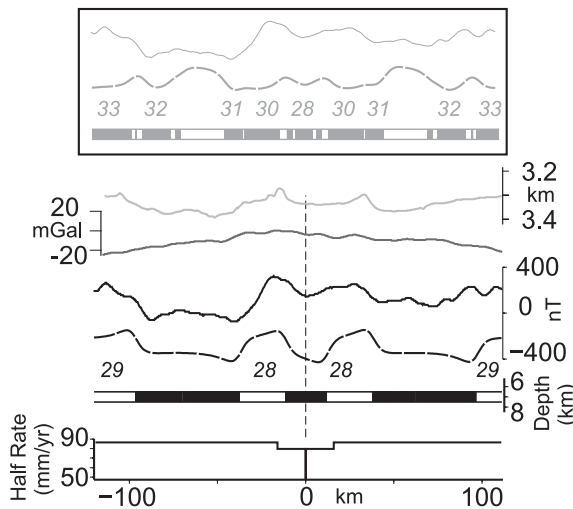


**Figure 4.** Bottom: Laxmi basin magnetic model based on a flat 1-km-thick source layer at 6.5 km depth, recorded in its present location and initially formed in the southern hemisphere. Model profile (dashed line) is compared to a ship track magnetic profile across the basin (solid line, location in Fig. 1). Gravity (mid grey) and bathymetry (light grey) are also shown. Top: an alternative model for spreading at 84–63 Ma in the Laxmi basin made using very slow ( $<10 \text{ mm yr}^{-1}$ ) spreading rates, after Bhattacharya *et al.* (1994). All profiles projected onto N045°E.

28, which was probably preceded by extension of transitional crust during chron 30.

## INDIAN PLATE MOTION AND DRIVING TORQUES

van Hinsbergen *et al.* (2011) used two geodynamic models to examine the tilting and dragging effects of the arrival and expansion of the mantle plume heads on the speed of the Indian plate. One of the models examined viscous drag effects only, showing modest ( $15\text{--}30 \text{ mm yr}^{-1}$ ) overall speed increases to build up rapidly in the 2 Myr prior to plume head arrival, and subsequently to decay over a period of 25 Myr. The other model suggested the so-called downhill force introduced by tilting of the plate above the plume head may be of equal importance as the effect of viscous drag. The models also showed that these torques are greatest when applied by a plume head arriving beneath the plate's edge.

van Hinsbergen *et al.* (2011) compared their modelling results to Cretaceous and Paleogene rates of Indian plate motion over the mantle, using a composite history of India–Africa plate motions built from the rotations of Cande *et al.* (2010), Molnar *et al.* (1988) and Torsvik *et al.* (2008), summed with rotation parameters for African plate motion over the mantle (O'Neill *et al.* 2005). They noted that the rotations show the speed of the Indian plate to increase abruptly at 89 Ma to near the estimated  $\sim 80 \text{ mm yr}^{-1}$  upper-mantle slab-sinking ‘speed limit’ (Goes *et al.* 2008) by an amount that is entirely attributable to the arrival of the Morondava–Marion plume beneath the plate's southwestern edge. This change, however, appears to be a resolution effect. Our rotation set (Table 2) depicts plate motion in the period between chronos 34y and 28 using seven rotations, as opposed to van Hinsbergen *et al.*'s (2011) two, and reveals a smooth increase from initially sedate motion at 89 Ma until the ‘speed limit’ is reached around 71 Ma (Fig. 5). This pattern is not consistent with the arrival of the Morondava–Marion plume having introduced significant plate driving torques of its own.

Both rotation sets show that the speed of upper-mantle slab sinking is spectacularly exceeded at 68 Ma, resulting in a doubling or more of the Indian plate's speed over the mantle. As van Hinsbergen *et al.* (2011) noted, because of its abruptness, timing and magnitude, this increase is partially attributable to the application of viscous drag and gravitational tilting forces upon arrival of the Deccan–Réunion plume. Unlike van Hinsbergen *et al.*'s (2011) set,

**Table 2.** Rotation parameters for Africa and India plates in the moving hotspot reference frame.

Africa-hotspots to 61 Ma*			India-hotspots to 61 Ma**			
long	lat	Ang	long	lat	ang	Label
161.05	8.54	0.10	−168.84	−12.67	0.65	27ny
160.84	8.15	0.33	−165.94	−14.84	2.30	28ny
161.25	8.78	0.49	−166.77	−13.94	3.41	28no
160.91	8.24	0.65	−166.40	−14.41	5.54	29no
160.92	8.36	0.76	−162.04	−12.85	7.48	30ny
161.04	8.48	1.05	−162.57	−14.30	10.34	30no
161.02	8.46	1.21	−163.85	−15.74	11.13	31no
161.47	9.08	1.55	−164.66	−16.98	13.06	32n.1ny
162.19	10.16	1.97	−166.60	−18.22	14.52	33ny
163.15	11.44	2.93	−175.32	−24.21	15.64	33no
164.16	12.85	3.67	−178.61	−25.52	16.80	34ny
165.02	14.06	4.49	−178.23	−26.72	18.15	FIT
161.12	−9.67	17.82	−164.62	−14.94	32.04	120 Ma

\*Interpolated from rotations in O'Neill *et al.* (2005)

\*\*By summation of Africa-hotspots rotations with those in Table 1

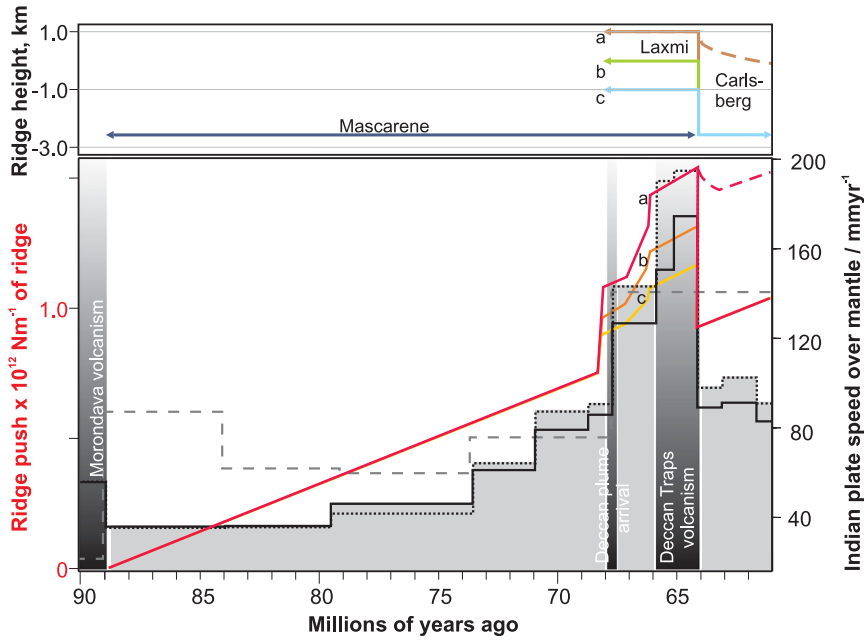


**Figure 5.** Top panel: assumed ridge crest depths and locations for modelling ridge push. Bottom panel: ridge push correlations with Indian plate speed over the mantle. Indian plate motion (solid-shaded region) over the mantle is shown based on rotations in Table 2 until 54°E, 10°S (solid black line) and 52°E, 25°S (dotted black line), two points on the boundary at 61 Ma. For comparison, the dashed grey line shows motion according to the rotations used by van Hinsbergen *et al.* (2011) until 54°E, 10°S. Coloured lines: ridge push calculated as described in the text (red/a: Laxmi Basin ridge at 1000 m depth, orange/b: Laxmi Basin ridge at sea level, yellow/c: 1000 m subaerial Laxmi Basin ridge).

however, at 64 Ma, our higher-resolution set of rotations shows that the speed of the Indian plate decreases to its pre-68 Ma value with an abruptness that is quite unlike the modelled slow decay of the effects of viscous drag by an expanding plume head. One possible explanation for this is that the material flux in the Deccan–Réunion plume stem was a much smaller fraction of that in its head than in either of the geodynamic models. We do not test or further consider this or other possibilities related to the viscous and downhill force mechanisms, which for the following we will instead assume to have changed at rates that were slow enough to disregard.

An alternative mechanism is that plume arrival reduced the viscous strength of the upper mantle, and hence led plate speed to increase by reducing its basal resistance to sliding (Kumar *et al.* 2007). A testable corollary of this alternative is that plate speed under such conditions should show enhanced sensitivity to changes in plate boundary forces, which unlike plume-arrival forces can indeed occur abruptly on geological timescales. Of such changes, the end of subduction could lead to an abrupt decrease in subduction-related torques as the descending slab is left to interact with the surface plate solely via the mantle flow it induces. Reconstructions of the subducted parts of the Indian plate, however, show ongoing subduction through late Cretaceous and Paleogene times (Hafkenscheid *et al.* 2006). Alternatively, lengths of divergent plate boundary can initiate and be abandoned over very short timescales by jumping or propagation. The Cretaceous and Paleogene Indian plate had a divergent boundary with the Antarctic plate that was situated in what is now the Bay of Bengal, where details of its possible interaction with the Kerguelen plume stem are poorly known (Duncan 2002; Gibbons *et al.* 2013). On the other hand, the Indian plate's southwestern divergent boundary, with the African plate, underwent major changes during this period. As shown above, the first relocation occurred during chron 30 along with the Deccan Traps volcanic phase, and was by more than 600 km northeastwards towards the Indian mar-

gin. It initiated the Laxmi Basin. The second, near the end of chron 28, was by ~100 km back southwestwards into the Laxmi Basin's margin, initiating part of the Carlsberg Ridge.

To examine whether changes to the Indian plate's divergent margins might have affected Indian plate motion, we completed simple calculations of the gravitational torque known as ridge push using the formulation of Richter & McKenzie (1978). The formulation describes the force that would tend to cause the lithosphere to slide down its own sloping base. Because of this slope, ridge push is proportional to plate thickness ( $L$ , here according to a half-space model as formulated by Turcotte & Schubert 2002) and the elevations of its ridge crests over the abyssal plains ( $e$ , according to the relationships of Stein & Stein 1992) according to

$$F_{RP} = ge(\rho_m - \rho_w)(L/3 + e/2)$$

(in which  $\rho_m$  and  $\rho_w$  are the mean densities of lithospheric mantle and seawater). We restricted our calculations to lithosphere formed along the divergent plate boundary at the southwestern edge of the Indian plate, given the low-resolution understanding of the co-evolution of the Indian–Antarctic ridge and Kerguelen Plateau.

Our assumptions about the evolution of these parameters along with that of the India–Africa plate boundary are summarized in Fig. 5. Starting at 89 Ma, the ridge crest and abyssal plains of the young Mascarene Basin would have been shallow, and its lithosphere thin, regardless of the presence, or otherwise, of Morondava–Marion plume mantle. For simplicity, we assume a 2.6-km deep ridge operating over normal-temperature mantle, in view of the cool crust and/or columnar mantle upwelling system implied by closely-spaced fracture zones near the margin (Bell & Buck 1992; Phipps Morgan & Parmentier 1995). We assume that first boundary relocation, from the Mascarene to the Laxmi basin at chron 30, occurred by ridge crest propagation into 30 Myr old Indian plate lithosphere, and that this occurred rapidly enough to preserve the lithospheric

thickness appropriate to such an age on the Indian flank of the new ridge. The resulting Laxmi Basin came to occupy 30 per cent of the boundary's total length. We are confident that the ridge in the Laxmi Basin operated over plume mantle. By analogy with plume-affected plate boundaries in the Afar Rift and Iceland, and in view of the seismic observations of fossil lava deltas in the north of the basin (Corfield *et al.* 2010; Calvès *et al.* 2011), we assume that the ridge was 1 km deep, or at sea level, or 1 km above sea level. The second boundary relocation occurred by rapid propagation of the Carlsberg Ridge into the Seychellois margin of the Laxmi Basin. Minshull *et al.* (2008) showed that this margin hosts only minor seaward dipping reflector sequences, and flanks oceanic crust of fairly normal (5–7 km) thickness, suggesting melting of non-plume mantle and a 'normal' depth of ~2.6 km for the Carlsberg Ridge. For comparison purposes, we also calculated ridge push for a Carlsberg Ridge subsiding from 1 km above sea level according to a half-space model for cooling of hot (1500°C) mantle. Finally, we assumed that the abandoned Mascarene and Laxmi ridges would cease to exert ridge push forces on the Indian plate by virtue of their incorporation into plate interiors along with their formerly-opposing flanks at which equal and opposite ridge push forces were raised.

Fig. 5 shows the results of calculating ridge push according to these considerations, and compares them to the changing speed of the Indian plate. Beginning at 89 Ma, ridge push increases linearly as the Mascarene Basin's abyssal plain deepens and its lithosphere thickens. This increase accompanies steady acceleration of the Indian plate over the mantle for the next 23 Myr. Upon relocation of part of the boundary to the Laxmi Basin during chron 30, with its already-thick lithosphere but shallower axis, calculated ridge push increases by 150–200 per cent. We modelled a stepwise increase, assuming that the ridge crest occupied the Laxmi Basin by propagation in stages, as opposed to a wholesale jump. The increase coincides with doubling of the speed of the Indian plate over the mantle. When the Laxmi Basin is abandoned and the plate boundary relocates to the deeper Carlsberg Ridge, the value of ridge push reverts onto the linear trend for a 2.6-km deep ridge and its flanks that started at 89 Ma. Illustrating the importance of rapid changes in ridge depth by propagation over areas of differing mantle, ridge push for a subsiding, initially 1 km subaerial ridge does not show a sharp reduction to coincide with the reduction in plate speed.

These correlations indicate a finely-balanced set of torques in which ridge push has the potential to play a large role in driving plate motion in spite of the order-of-magnitude greater buoyancy of subducting slabs. As physical and mathematical models have suggested, this may be because less than 10 per cent of slabs' buoyancy is transmitted around the subduction hinge (Schellart 2004; Sandiford *et al.* 2005; Husson 2012). Schellart (2004) went on to conclude that because of this, the effective plate driving torque from slab buoyancy was just twice that of ridge push. Our simply-modelled increase in ridge push thus implies a considerable increase in effective plate boundary torques on the Indian plate at 68–64 Ma. These considerations add to existing plate kinematic indications that ridge push was able to balance waning subduction-related torques later in the plate's history (Copley *et al.* 2010).

To summarize, we interpret the plate kinematic record from the Mascarene and Laxmi basins to infer that the Deccan–Réunion plume served to increase the speed of the Indian plate by virtue of its combined influences on the mid-ocean ridge at the Indian–African plate boundary and the viscosity just below the base of the plate. The ridge crest relocated over the arriving plume head, increasing the Indian plate's gravitational potential by raising part of its edge at the same time as the spread of plume material in the upper

mantle reduced basal drag on the Indian lithosphere. As it does not need to involve changes in the long-wavelength topography at the base of the lithosphere by wholesale plate tilting, this mechanism differs from the downhill force modelled elsewhere. Furthermore, our results constitute plate kinematic evidence for a setting in which the effective magnitudes of ridge push and slab pull forces were similar to one another.

## ACKNOWLEDGEMENTS

We thank Royal Holloway University of London for support. We are grateful for constructive reviews by Laurent Husson and one anonymous reviewer that prompted improvements to the manuscript.

## REFERENCES

- Becker, T.W. & Faccenna, C., 2011. Mantle conveyor beneath the Tethyan collisional belt, *Earth planet. Sci. Lett.*, **310**, 453–461.
- Bell, R.E. & Buck, W.R., 1992. Crustal control of ridge segmentation inferred from observations of the Reykjanes Ridge, *Nature*, **357**, 583–586.
- Bernard, A. & Munschy, M., 2000. Were the Mascarene and Laxmi Basins (western Indian Ocean) formed at the same spreading centre? *Comptes Rendus de l'Acad. des Sci. – Ser. IIa – Earth planet. Sci.*, **330**, 777–783.
- Bhattacharya, G.C., Chaubey, A.K., Murty, G.P.S., Srinivas, K., Sarma, K., Subrahmanyam, V. & Krishna, K.S., 1994. Evidence for sea-floor spreading in the Laxmi Basin, northeastern Arabian Sea, *Earth planet. Sci. Lett.*, **125**, 211–220.
- Bridges, D.L., Mickus, K., Gao, S.S., Abdelsalam, M.G. & Alemu, A., 2012. Magnetic stripes of a transitional continental rift in Afar, *Geology*, **40**, 203–206.
- Calvès, G., Schwab, A.M., Huuse, M., Clift, P.D., Gaina, C., Jolley, D., Tabrez, A.R. & Inam, A., 2011. Seismic volcanostratigraphy of the western Indian rifted margin: the pre-Deccan igneous province, *J. geophys. Res.*, **116**, B01101, doi:10.1029/2010JB000862.
- Cande, S.C., Patriat, P. & Dymnt, J., 2010. Motion between the Indian, Antarctic and African plates in the early Cenozoic, *Geophys. J. Int.*, **183**, 127–149.
- Cande, S.C. & Stegman, D.R., 2011. Indian and African plate motions driven by the push force of the Réunion plume head, *Nature*, **475**, 47–52.
- Coblenz, D.D. & Richardson, R.M., 1995. Statistical trends in the intraplate stress field, *J. geophys. Res.*, **100**, 20 245–20 255.
- Collier, J.S., Sansom, V., Ishizuka, O., Taylor, R.N., Minshull, T.A. & Whitmarsh, R.B., 2008. Age of Seychelles–India break-up, *Earth planet. Sci. Lett.*, **272**, 264–277.
- Copley, A., Avouac, J.-P. & Royer, J.Y., 2010. India–Asia collision and the Cenozoic slowdown of the Indian plate: implications for the forces driving plate motions, *J. geophys. Res.*, **115**, B03410, doi:10.1029/2009JB006634.
- Corfield, R.I., Carmichael, S., Bennett, J., Akhter, S., Fatimi, M. & Craig, T., 2010. Variability in the crustal structure of the West Indian Continental Margin in the Northern Arabian Sea, *Petrol. Geosci.*, **16**, 257–265.
- Duncan, R.A. & Hargraves, R.B., 1990.  $^{40}\text{Ar}/^{39}\text{Ar}$  geochronology of basement rocks from the Mascarene Plateau, the Chagos Bank, and the Maldives Ridge, in *Proceedings of the ODP, Sci. Results*, Vol. 115, pp. 43–51, eds Duncan, R.A. *et al.*, College Station, TX (Ocean Drilling Program).
- Dymnt, J., 1991. Structure et evolution de la lithosphère océanique dans l'océan Indien: apport des anomalies magnétiques, *PhD thesis*, University of Louis Pasteur, Strasbourg, France, 374 pp.
- Duncan, R.A., 2002. A time frame for construction of the Kerguelen Plateau and broken ridge, *J. Petrol.*, **43**, 1109–1119.
- Eagles, G., 2003. Tectonic evolution of the Antarctic–Phoenix plate system since 15 Ma, *Earth planet. Sci. Lett.*, **217**, 97–109.
- Eagles, G. & Hoang, H.H., in review. Cretaceous to present kinematics of the Indian, African and Seychelles plates, *Geophys. J. Int.*
- Forsyth, D.W. & Uyeda, S., 1975. On the relative importance of the driving forces of plate motion, *Geophys. J. R. astr. Soc.*, **43**, 163–200.

- Ganerød, M. *et al.*, 2011. Palaeoposition of the Seychelles microcontinent in relation to the Deccan Traps and the Plume Generation Zone in Late Cretaceous-Early Palaeogene time, in *The Formation and Evolution of Africa: A Synopsis of 3.8 Ga of Earth History*, Vol. 357, pp. 229–252, eds Van Hinsbergen, D.J.J., Buiter, S.J.H., Torsvik, T.H., Gaina, C. & Webb, S.J., Geological Society, London, Special Publications.
- Gibbons, A.D., Whittaker, J.M. & Müller, R.D., 2013. The breakup of East Gondwana: assimilating constraints from Cretaceous ocean basins around India into a best-fit tectonic model, *J. geophys. Res.*, **118**, 808–822.
- Goes, S., Capitanio, F.A. & Morra, G., 2008. Evidence of lower-mantle slab penetration phases in plate motions, *Nature*, **451**, 981–984.
- Gradstein, F.M. *et al.*, 2004. *A Geologic Time Scale 2004*, Cambridge University Press, Cambridge, 589 pp.
- Gurnis, M. & Torsvik, T.H., 1994. Rapid drift of large continents during the late Precambrian and Paleozoic: paleomagnetic constraints and dynamic models, *Geology*, **22**, 1023–1026.
- Hafkenscheid, E., Wortel, M.J.R. & Spakman, W., 2006. Subduction history of the Tethyan region derived from seismic tomography and tectonic reconstructions, *J. geophys. Res.*, **111**, B08401, doi:10.1029/2005JB003791.
- Husson, L., 2012. Dynamics of plate boundaries over a convective mantle, *Phys. Earth planet. Inter.*, **212**, 32–43.
- Krishna, K.S., Gopala Rao, D. & Sar, D., 2006. Nature of the crust in the Laxmi Basin ( $14^{\circ}$ – $20^{\circ}$ N), western continental margin of India, *Tectonics*, **25**, TC1006, doi:10.1029/2004TC001747.
- Kumar, P., Yuan, X., Kumar, M.R., Kind, R., Li, X. & Chadha, R.K., 2007. The rapid drift of the Indian tectonic plate, *Nature*, **449**, 894–897.
- Lawver, L.A., Gahagan, L.M. & Dalziel, I.W.D., 1998. A tight fit early Mesozoic Gondwana: a plate reconstruction perspective, *Mem. Natl. Inst. Pol. Res. Spec. Issue*, **53**, 214–229.
- Livermore, R.A., Nankivell, A.P., Eagles, G. & Morris, P., 2005. Paleogene opening of Drake Passage, *Earth planet. Sci. Lett.*, **236**, 459–470.
- Masson, D.G., 1984. Evolution of the Mascarene Basin. Western Indian Ocean, and significance of the Amirante Arc, *Mar. Geophys. Res.*, **6**, 365–382.
- Minshull, T.A., Lane, C.L., Collier, J. & Whitmarsh, R.B., 2008. The relationship between rifting and magmatism in the northeastern Arabian Sea, *Nat. Geosci.*, **1**, 463–467.
- Molnar, P., Pardo-Casas, F. & Stock, J., 1988. The Cenozoic and Late Cretaceous evolution of the Indian Ocean: uncertainties in the reconstructed positions of the Indian, African and Antarctic plates, *Basin Res.*, **1**, 23–40.
- Müller, R.D., Gaina, C., Roest, W. & Hansen, D.L., 2001. A recipe for microcontinent formation, *Sedology*, **29**, 203–206.
- O'Neill, C., Müller, R.D. & Steinberger, B., 2005. On the uncertainties in hot spot reconstructions and the significance of moving hot spot reference frames, *Geochem. Geophys. Geosyst.*, **6**, Q04003, doi:10.1029/2004GC000784.
- Phipps Morgan, J. & Parmentier, E.M., 1995. Crenulated seafloor: evidence for spreading rate dependent structure of mantle upwelling and melting beneath a mid-oceanic spreading center, *Earth planet. Sci. Lett.*, **129**, 73–84.
- Richter, F.M. & McKenzie, D., 1978. Simple plate models of mantle convection, *J. Geophys.*, **44**, 441–471.
- Sandiford, M., Coblenz, D. & Schellart, W.P., 2005. Evaluating slab-plate coupling in the Indo-Australian plate, *Geology*, **33**, 113–116.
- Sandwell, D.T. & Smith, W.H.F., 2009. Global marine gravity from retracked Geosat and ERS-1 altimetry: ridge segmentation versus spreading rate, *J. geophys. Res.*, **114**, B01411, doi:10.1029/2008JB006008.
- Schellart, W.P., 2004. Quantifying the net slab pull force as a driving mechanism for plate tectonics, *Geophys. Res. Lett.*, **31**, L07611, doi:10.1029/2004GL019528.
- Stein, C. & Stein, S., 1992. A model for the global variation in oceanic depth and heat flow with lithospheric age, *Nature*, **359**, 123–128.
- Storey, M., Mahoney, J.J. & Saunders, A.D., 1997. Cretaceous basalts in Madagascar and the transition between plume and continental lithosphere mantle sources, in *Large Igneous provinces: Continental, Oceanic, and Planetary Flood Volcanism*, pp. 95–122, eds Mahoney, J.J. & Coffin, M., Am. Geophys. Union, Monogr., Washington, DC.
- Torsvik, T.H., Ashwal, L.D., Tucker, R.D. & Eide, E.A., 2001. Neoproterozoic geochronology and palaeogeography of the Seychelles microcontinent: the India link, *Precambrian Res.*, **110**, 47–59.
- Torsvik, T.H., Müller, R.D., Van der Voo, R., Steinberger, B. & Gaina, C., 2008. Global plate motion frames: toward a unified model, *Rev. Geophys.*, **46**, RG3004, doi:10.1029/2007RG000227.
- Torsvik, T.H. *et al.*, 2013. A Precambrian microcontinent in the Indian Ocean, *Nature Geosci.*, **6**, 223–227.
- Turcotte, D.L. & Schubert, G., 2002. *Geodynamics*, 2nd edn, Cambridge University Press, Cambridge, UK.
- van Hinsbergen, D.J.J., Steinberger, B., Doubrovine, P.V. & Gassmöller, R., 2011. Acceleration and deceleration of India-Asia convergence since the Cretaceous: roles of mantle plumes and continental collision, *J. geophys. Res.*, **116**, B06101, doi:10.1029/2010JB008051.